



ELSEVIER

Marine Geology 220 (2005) 23–40

**MARINE  
GEOLOGY**

INTERNATIONAL JOURNAL OF MARINE  
GEOLOGY, GEOCHEMISTRY AND GEOPHYSICS

www.elsevier.com/locate/margeo

## Downward particle fluxes in the Guadiaro submarine canyon depositional system (north-western Alboran Sea), a river flood dominated system

Albert Palanques<sup>a,\*</sup>, Mohamed El Khatab<sup>a</sup>, Pere Puig<sup>a</sup>, Pere Masqué<sup>b</sup>,  
Joan Albert Sánchez-Cabeza<sup>c</sup>, Enrique Isla<sup>a</sup>

<sup>a</sup> Institut de Ciències del Mar (CSIC), Passeig Marítim de la Barceloneta, 37–49, E-08003 Barcelona, Spain

<sup>b</sup> Institut de Ciència i Tecnologia Ambientals, Departament de Física, Universitat Autònoma de Barcelona, E-08193 Bellaterra, Spain

<sup>c</sup> International Atomic Energy Agency, Marine Environment Laboratory, 4 Quai Antoine 1er, 98000 Monaco

Received 11 May 2004; received in revised form 5 July 2005; accepted 15 July 2005

### Abstract

Three moorings equipped with sediment traps were deployed in the north-western Alboran continental margin to study downward particle fluxes in the Guadiaro submarine canyon depositional system. This area is located close to the Strait of Gibraltar and is influenced by the upwelling induced by the Atlantic Jet and by episodic flood events from the Guadiaro River. Sediment traps were installed in the Guadiaro Canyon, in the Guadiaro Channel and in the adjacent continental slope. The overall duration of the deployment was 12 months (from November 1997 to October 1998). Time-series of downward particle fluxes, major constituents (organic carbon, nitrogen, biogenic opal, calcium carbonate and lithogenics) and <sup>210</sup>Pb were determined near the surface at mid-depths and near the bottom. Total mass fluxes (TMF) in this area fluctuated more than two orders of magnitude and showed an important seasonal variability with higher fluxes in winter. Increases in TMF and lithogenics together with decreases in <sup>210</sup>Pb, organic carbon and opal were recorded in all traps coinciding with river floods, indicating a direct response of the system to these events and a rapid offshore transport of suspended matter affecting the entire water column. The channel site received similar particle fluxes to the western open slope site, indicating that this channel did not act as a preferential sediment conduit during the deployment period. In the Guadiaro Canyon, TMF were more than one order of magnitude higher, <sup>210</sup>Pb concentration was lower (one half) and organic matter was more degraded than at the channel site during spring and summer, as a consequence of receiving particles resuspended by internal waves and occasionally by trawling activities. These particles were mainly retained in the canyon, which works as a trap. Also, during spring and summer, the opal and organic carbon percentages increased in all traps both in magnitude and variability, and peaks seem to be associated with biological blooms.

© 2005 Elsevier B.V. All rights reserved.

**Keywords:** submarine canyon; downward particle fluxes; Alboran Sea; sedimentary processes; <sup>210</sup>Pb

\* Corresponding author. Tel.: +34 932309500; fax: +34 932309555.

E-mail address: albertp@icm.csic.es (A. Palanques).

## 1. Introduction

Spatial and temporal estimations of particle fluxes using sediment traps have been studied in several continental margins of the world (e.g., Deuser, 1986; Biscaye et al., 1988; Monaco et al., 1990; Biscaye and Anderson, 1994; Puig and Palanques, 1998; Thunel, 1998; De Lazzari et al., 1999; Heussner et al., 1999; Walsh and Nittrouer, 1999; Palanques et al., 2002). The main objective of these studies was to understand the continent–ocean particle transfer and to determine its role in the marine biogeochemical cycles. In general, the continental margins are regions characterised by sediment inputs from the continent and by high primary production which sequesters atmospheric carbon, and they therefore have an important effect on global biogeochemical cycles (Walsh et al., 1988; Walsh, 1991). However, there is a high diversity of sedimentary regimes, not only among continental margins, but also within each continental margin itself, particularly in those with canyon-incised slopes. The study of downward particle fluxes in submarine canyons has revealed their role as preferential conduits of matter between the shallow and deep environments (Gardner, 1989; Monaco et al., 1990; Puig and Palanques, 1998; Heussner et al., 1999; Palanques et al., 2005). Several of these studies found relationships between storms and river flood events and increases in particle fluxes, although these relationships have not always been evident. Therefore, it is still necessary to study sediment fluxes in different geological contexts in order to better understand the mechanisms that control particle fluxes in submarine canyons. One specific area characterised by the presence of several submarine canyons where canyon particle fluxes have not yet been studied is the north-western Alboran Margin.

Previous studies on particle fluxes in the Alboran Sea include an indirect estimation of the interchange of carbon through the Gibraltar Strait (Copin-Montegut and Avril, 1993; Dafner et al., 2001) and short-term particle flux measurements (Peinert and Miquel, 1994; Dachs et al., 1996, 1998). Downward particle fluxes on the open slope off Malaga and in the western deep Alboran basin have recently been studied by Fabres et al. (2002) and Masqué et al. (2003). However, none of these studies focused on the role

that submarine canyons play at present in the Alboran Sea. The main objective of this work is to study the temporal evolution of downward particle fluxes and their major constituents in a submarine canyon depositional system of the northwestern Alboran margin. Among the several canyon systems of this margin, the Guadiaro submarine canyon depositional system was chosen because: (1) it is linked to one of the few small rivers of this basin not affected by dams, with continuous water discharge and sporadic flood events, (2) it is in a margin with a very narrow shelf where direct response between floods and cross-margin sediment transfer is expected, and (3) it is in an upwelling zone where increases in productivity take place.

## 2. Regional setting

The Alboran Sea is an epicontinental sea adjacent to the Gibraltar Strait (Fig. 1) and surrounded by continental margins where small rivers discharge, relatively short submarine canyons develop (Ercilla et al., 1992; Alonso and Ercilla, 2003) and high productivity occurs (Rodríguez et al., 1994, 1998; Sarhan et al., 2000; Moran and Estrada, 2001). The climatic regime in the Alboran Sea shows a well-defined seasonal pattern with rains in autumn and winter and dry periods in spring and summer. Some of the small rivers discharging into the Alboran Sea, such as the Guadiaro and the Guadalhorce, have a continuous water discharge during the year, while others, such as the Guadalmedina, Fuengirola, Manilva and Verde, are characterised by smaller and irregular discharges.

The oceanography of the western Alboran basin is influenced by the Atlantic Jet (AJ) that enters the Alboran Sea through the Strait of Gibraltar and forms a large anticyclonic gyre in this basin, known as the Western Alboran Gyre (WAG) (Heburn and La Violette, 1990; Tintoré et al., 1991; Viúdez et al., 1996; Millot, 1999; Baldacci et al., 2001). The AJ shows important variations in its orientation, fluctuating in a north–south direction (Sarhan et al., 2000). The southward drifting of the AJ and the winds generate an upwelling region in the northern part of the WAG that favours the fertilisation of the photic layer (Gil and Gomis, 1994; Packard et al., 1988; Garcia-

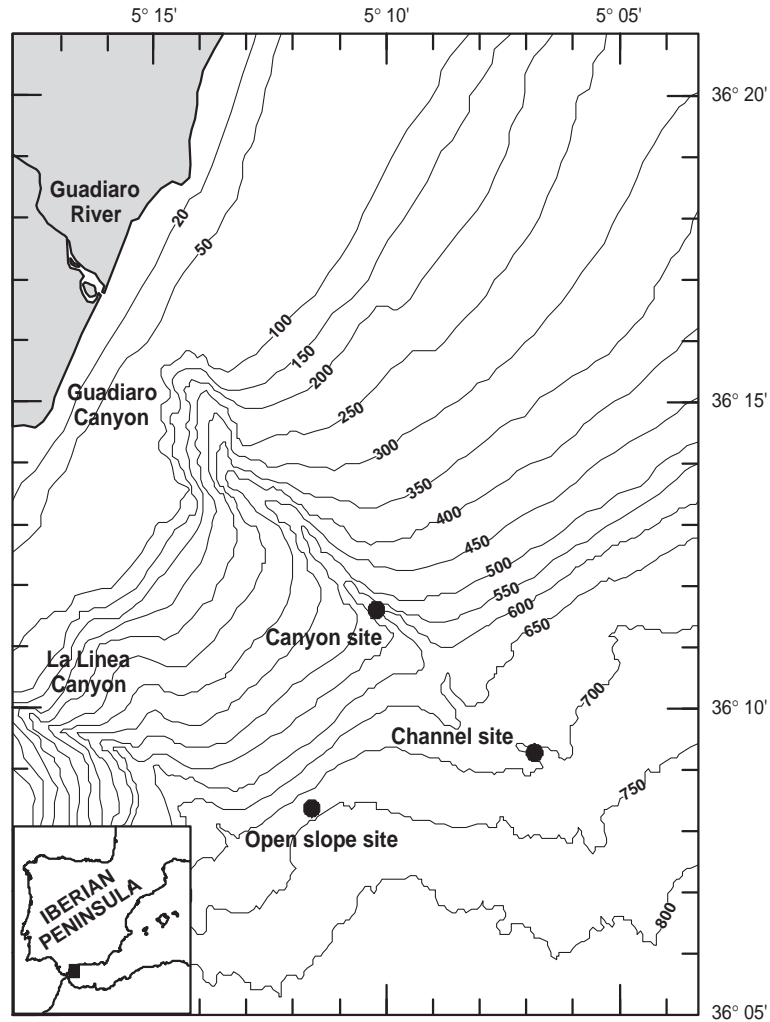


Fig. 1. Map showing the bathymetry of the study area and the incisions of the Guadiaro and La Linea submarine canyons. The locations of the moorings are indicated by “canyon site”, “channel site”, and “open slope site”.

Górriz and Carr, 1999; Sarhan et al., 2000; Rubin et al., 1992).

The study area, in the north-western Alboran margin, is incised by the Guadiaro Canyon and also by La Linea Canyon towards the west (Fig. 1). This area is located northward from the AJ, which usually has a more centred position in the basin and is therefore under the influence of the upwelling zone. Associated with the fluctuation of the AJ, a cyclonic gyre develops close to the coast in the Guadiaro continental shelf, forming an anti-clockwise cell characterised by less intense currents flowing towards the Strait of Gibraltar (García Lafuente and Cano Lucaya, 1994).

The continental shelf in the proximity of the Guadiaro Canyon is the narrowest in the north-western Alboran margin, with an average width of 4 km and a steep gradient of  $0.06^\circ$ . The continental slope is also narrow, being about 10 km wide with a gradient of  $0.8^\circ$ . The base-of-slope starts at about 600 m water depth and extends to 945 m depth with a gradient of less than  $0.2^\circ$  (Ercilla et al., 1992). The Guadiaro Canyon head is 4.5 km off the Guadiaro River mouth and the shelf-break at the canyon head is at 70 m depth. The direction of this canyon is NW–SE, showing an average incision of 100 m depth. The axial gradient along the Guadiaro

Canyon decreases from 7° at the canyon head to 2° at the canyon mouth. At the base-of-slope the canyon evolves to a leveed-channel that extends down to 750 m water depth and a turbidite system develops. (Alonso and Ercilla, 2003).

### 3. Material and methods

Three mooring arrays equipped with pairs of sediment traps and current meters were deployed in the Guadiaro Canyon depositional system: one in the lower part of the submarine canyon, another in the turbiditic channel and the third on its western adjacent slope (Fig. 1), hereafter referred to as the canyon, channel and open slope sites. The mooring at the canyon site was deployed in the axis of the canyon at 592 m depth, near the canyon mouth, with one set of instruments placed at 25 m above the seafloor. The mooring at the channel site was deployed at 717 m depth and included three sets of instruments: at 25 m above the seafloor (near-bottom), at 500 m depth (intermediate waters), and at 135 m depth (near-surface). The open slope mooring was located westward from the Guadiaro Canyon at 720 m water depth, and included one set of instruments placed at 25 m above bottom. The total sampling period comprised 348 days divided into two deployment periods: from 1 November 1997 to 11 May 1998 and from 20 May 1998 to 22 October 1998, with a 9-day gap (11–20 May 1998) due to recovery and re-deployment operations. During the first deployment period, the sampling intervals of the sediment traps were 16 days long, whereas during the second period the first four sampling intervals were 7 days and the remaining 16 days long.

After the first deployment, the channel and open slope moorings were recovered, but not the canyon mooring, which was lost presumably due to an accident caused by fishing activities. During the second deployment, the instruments installed previously at the slope site were moved to the canyon site in order to collect measurements within the canyon, at least for half of the study period. We thus obtained data from the three instrumented levels of the channel site during a complete year, data from the near-bottom instruments at the open slope site during the Novem-

ber 97–May 98 period and data from the near-bottom instruments at the canyon site during the May 98–October 98 period.

The sediment traps used in this study were Technicap PPS/3 traps, which have a collecting area of 0.125 m<sup>2</sup> and a sequential rotating carousel with 12 cups (Heussner et al., 1990), and the current meters were the first generation of Aanderaa RCM9 equipped with a Doppler sensor. To prevent sample degradation, the sediment trap collecting cups were filled with a 5% (~1.7 M) formalin solution (40% formaldehyde mixed with 0.2 µm of filtered seawater) before their deployment. According to Heussner et al. (1990), swimmers were removed by wet sieving on a 1 mm nylon mesh and hand-picking under a dissecting microscope. The total sample was divided with a peristaltic pump into several homogeneous aliquots. To determine total mass flux, four sub-samples were filtered through pre-weighed, rinsed (with distilled water) and dried (overnight at 40 °C) Millipore cellulose acetate filters (0.45 µm pore size, 47 mm diameter). Total mass fluxes were calculated from the sample dry weight, the collecting trap area and the sampling interval.

To determine total carbon (TC), organic carbon (OC) and nitrogen (N) concentration, six sub-samples were filtered onto pre-weighed and pre-combusted (overnight at 550 °C) Whatman GF/F glass microfibre filters (47 mm diameter). Two subsamples were used to determine the TC and N in a LECO CN 2000 analyser. The inorganic carbon (IC) was obtained by acid digestion (HCl 6M) of another two sub-samples in a LECO CC-100 connected to the CN analyser. The difference between the TC and IC was considered OC. The calcium carbonate (CaCO<sub>3</sub>) was calculated by multiplying IC by 8.33.

The biogenic silica (opal) concentration was obtained using a wet-alkaline extraction with sodium carbonate according to the Mortlock and Froelich (1989) method, modified for small trap samples (Biscaye and Anderson, 1994).

The lithogenic fraction was defined as the difference between the total mass and the sum of the biogenic constituents [organic matter (twice the weight of organic carbon), calcium carbonate and opal].

<sup>210</sup>Pb analyses were performed following the methodology described by Sánchez-Cabeza et al.

(1998), assuming that  $^{210}\text{Pb}$  was in secular equilibrium with its daughter radionuclide  $^{210}\text{Po}$ . An aliquot of each sample was spiked with  $^{209}\text{Po}$  and totally digested using an analytical microwave oven. After digestion, samples were made 1 N HCl and  $^{209}\text{Po}$  and  $^{210}\text{Po}$  were deposited onto silver disks, previously coated on one side with a plastic lacquer, and left at 60–70 °C for 8 h while stirring. Polonium isotopes were counted with  $\alpha$ -spectrometers equipped with low-background SSB surface barrier detectors in vacuum conditions (EG and G Ortec).

Mean fluxes and mean concentrations of constituents were estimated as time-weighted mean fluxes and flux-weighted mean concentrations (Heussner et al., 1990; Biscaye and Anderson, 1994), which is equivalent to what had been collected by a single cup during the entire mooring deployment time.

Time series of Guadiaro River water discharge were facilitated by the “Confederación Hidrográfica del Sur” and measured daily at the gauging station from San Pablo de Buceite, located 25 km upstream of the river mouth. Significant wave height was supplied by “Puertos del Estado” and recorded hourly by a hydrographical buoy located at 585 m water depth (36°13.8'N 5°1.8'W) about 16 km eastward from the Guadiaro Canyon. Additional information about currents in surface and intermediate waters during the study period was also supplied by “Puertos del Estado”. Currents were recorded at approximately 150 and 500 m water depth on a mooring line located at 4°59.7'W, 36°13.0'N at 704 m water depth, about 10 km away from the study area.

## 4. Results

### 4.1. Total mass fluxes

The temporal series of the total mass fluxes (TMF) are represented in Fig. 2. The TMF showed great variability, ranging more than two orders of magnitude (from 101 to 27397  $\text{mg m}^{-2} \text{d}^{-1}$ ).

At the Guadiaro channel site, TMF decreased from the autumn–winter period to the spring–summer period at the three depths. At this site, the higher TMF peaks (up to 5669  $\text{mg m}^{-2} \text{d}^{-1}$ ) occurred near the bottom and at 500 m depth in late December and in

February, whereas at 135 m they occurred in November and also in late December. An isolated TMF peak took place in August at 500 m depth. The lowest TMF (down to 101  $\text{mg m}^{-2} \text{d}^{-1}$ ) took place at 135 and 500 m depth in June and July and near the bottom in September (Fig. 2a, b and c). In relation to the upper level, the mean TMF increased with depth by a factor of 1.6 in the mid-water level and by 2.3 near the bottom.

At the open slope site, the near-bottom TMF trend during the autumn–winter period was relatively similar to that of the channel site, but the mean TMF at the open slope site was about 1.2 times higher than that of the channel site (Fig. 2c and d; Table 1B). TMF at the open slope site increased in December reaching maximum values over 6000  $\text{mg m}^{-2} \text{d}^{-1}$  both in early December and in late December. Other TMF increases were in November and in February (Fig. 2d). The December near-bottom peak was stronger on the open slope than in the channel but the February peak was weaker.

In the Guadiaro submarine canyon, near-bottom TMF during the spring–summer period were much higher than at the other sites, the mean value being 8 times higher than those at the channel site (Table 1C). Very strong TMF peaks occurred in late May and in mid-July (Fig. 2e). The May peak correspond to the highest TMF recorded in the study area.

### 4.2. Currents

The current meters used in this study were the very first version of the Aanderaa RCM9 model. Unfortunately, due to the low concentrations of suspended particles in the water at the study sites, scattering was insufficient for the correct functioning of this early version of the acoustic Doppler sensor. Recorded currents were only reliable in the near-bottom waters of the canyon site, where suspended particulate matter concentrations were higher. For this reason, the current regime at the near-surface (135 m) and mid-depth (500 m) trap levels during the study period was obtained from current meter data supplied by “Puertos del Estado”. The currents at 150 m water depth showed maximum current velocities of 42 cm/s, with tidal peak velocities of between 20 and 30 cm/s most of the time, whereas current velocities at 500 m water depth reached

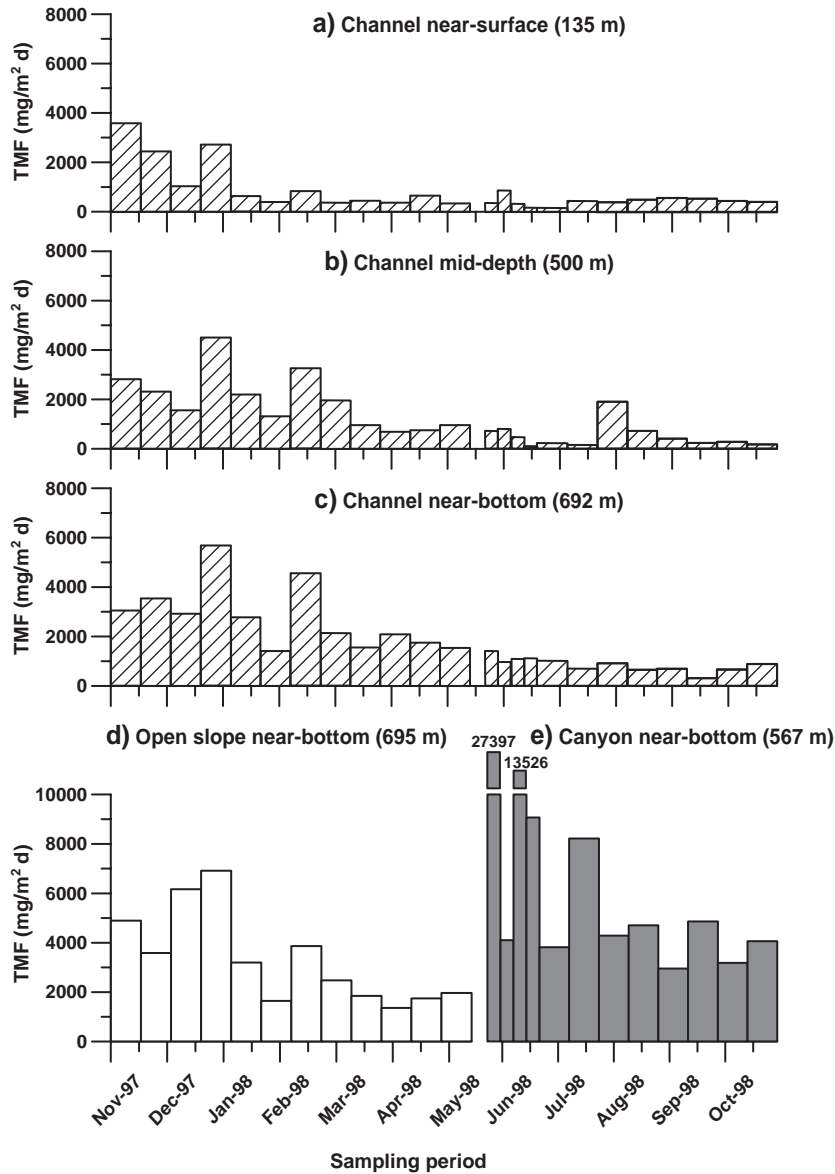


Fig. 2. Time series of the total mass fluxes of particulate matter collected in the Guadiaro Canyon depositional system during this study. The gap between May and June was due to recovery and deployment between the first and the second sampling period.

maximum values of only 18 cm/s. Near the bottom at the canyon site, maximum velocities recorded by the Aanderaa RCM9 current meter during regular tidal cycles were about 20 cm/s.

According to the results obtained by Gardner et al. (1997), the collection efficiency of the type of sediment traps used in this study is not significantly affected by currents below 23 cm/s. Thus, sediment

traps installed at 500 m depth and near the bottom were not affected by bias, whereas the collection efficiency at 135 m water depth could be influenced by currents, and reported fluxes at this level should therefore be considered as semi-quantitative values. However, fluxes at 135 m depth are coherent with the fluxes measured at the other traps and do not alter the results of this paper.

### 4.3. Major constituents

Mean percentages and mean fluxes of major constituents of the downward particulate flux are presented in Tables 1A–1C, whereas the temporal series of major constituent percentages and fluxes during the study period are presented in Figs. 3 and 4. As deployment periods in the open slope and canyon sites are not the same, in this section we assume that the channel is compared with the open slope for the first period (November 97–May 98) and with the canyon for the second period (May 98–October 98). In general, fluxes of the major constituents (Fig. 4) followed the same pattern as the TMF (Fig. 2) because the variability of the TMF is much higher than the variability of the major constituents concentrations.

The OC concentration in all traps ranged from 1.4% to 8.1%. At the channel site, the variability, the maximum values and the mean values of the OC concentration during the year decreased with depth (Fig. 3a; Table 1A). OC percentages maintained similar low values during the autumn–winter period, with minimum concentrations in late December and February, but increased in spring and summer at all levels, and especially at 135 m, where there were significant peaks in late May, June and September. At the channel site the mean near-bottom OC concentration was similar to that at the open slope site (Fig. 3d; Table 1B) and significantly higher than that at the canyon site, showing a mean value twice that of the canyon (Fig. 3a; Table 1C). In general, the OC concentration in the downward particulate matter tended to decrease with depth in the water column, while near the bottom

it increased from the canyon to the channel site, where it was similar to that of the open slope site.

The CaCO<sub>3</sub> percentages ranged from 5.9% to 18.1%. At the channel site, maximum CaCO<sub>3</sub> percentages occurred at 135 m depth in late May and early June. At the open slope site, the near-bottom CaCO<sub>3</sub> percentage was slightly higher than at the channel site, with similar maximum and minimum concentrations (Table 1B; Fig. 3b). At the canyon site, the mean near-bottom CaCO<sub>3</sub> percentage was slightly higher than at the channel, showing similar maximum values and lower minimum values (Fig. 3b; Table 1C). Trends with depth changed during the deployment period (Fig. 3b), although the mean concentrations decreased with depth (Table 1A). Near the bottom it was relatively similar at the three study sites, with slightly lower values at the channel site.

Time series of opal percentage during the study period are represented in Fig. 3c. At the channel site, the opal concentration at the three depths showed lower and more homogeneous percentages during the autumn–winter period and higher and more variable percentages during the spring–summer period, when the mean opal concentration was twice that of the previous deployment period (Fig. 3c; Tables 1A–1C). Maximum opal concentrations at the channel site were around 12% in late May, late June and early August, while minimum concentrations occurred in November, late December and February. At the open slope site, the opal percentage was lower than at the channel (Table 1B) and the minimum values were in November and in late December, whereas the maximum was in late January. At the canyon site, the near-

Table 1A

Time-weighted mean fluxes of total mass and major constituents ( $\text{mg m}^{-2} \text{d}^{-1}$ ) and flux-weighted mean concentrations (wt.%) of major constituents of the sinking particles collected in the moored traps installed at the Guadiaro channel site during the two FLUXALB deployments made between 1 November 1997 and 22 October 1998 (almost one year period)

	Channel near-surface		Channel mid-depth		Channel near-bottom	
	Mean conc.	Mean flux	Mean conc.	Mean flux	Mean conc.	Mean flux
TMF	–	822.6	–	1302.4	–	1870.5
OC	2.9	24.2	2.5	32.4	2.2	40.5
N	0.4	3.6	0.3	4.5	0.3	5.4
CaCO <sub>3</sub>	13.2	108.5	12.4	161.5	11.7	218.7
Opal	5.0	41.4	5.5	71.6	5.4	101.3
Lithogenics	75.9	624.3	73.1	1004.5	78.6	1469.0
<sup>210</sup> Pb*	539.0	0.4	566.0	0.7	596.0	1.1

\*<sup>210</sup>Pb mean concentration is in Bq kg<sup>-1</sup> and <sup>210</sup>Pb mean fluxes in Bq m<sup>-2</sup> d<sup>-1</sup>.

Table 1B

Time-weighted mean fluxes of total mass and major constituents ( $\text{mg m}^{-2} \text{d}^{-1}$ ) and flux-weighted mean concentrations (wt.%) of major constituents of the sinking particles collected in the near-bottom traps installed at the Guadiaro channel and open slope sites between 1 November 1997 and 11 May 1998 (1st deployment period)

	Channel near-bottom (Nov 1997–May 1998)		Open slope near-bottom (Nov 1997–May 1998)	
	Mean conc.	Mean flux	Mean conc.	Mean flux
TMF	–	2744.2	–	3303.3
OC	1.9	54	1.8	60.4
N	0.2	7.1	0.2	7.6
CaCO <sub>3</sub>	11.7	321.9	12.5	413.1
Opal	4.7	129.7	3.5	115.1
Lithogenics	79.6	2260.2	80.3	2654.3
<sup>210</sup> Pb*	564.0	1.5	556	2.01

\*<sup>210</sup>Pb mean concentration is in  $\text{Bq kg}^{-1}$  and <sup>210</sup>Pb mean fluxes in  $\text{Bq m}^{-2} \text{d}^{-1}$ .

bottom opal percentage was lower than at the channel site, showing a mean concentration one third lower than there (Fig. 3c; Table 1C). Thus, the opal concentration did not decrease with depth and the maximum values were at the channel site. Opal was the major constituent that showed the greatest content variability and thus its flux (Fig. 4c) trend did not entirely coincide with that of TMF as it does for the other major constituents.

The lithogenic fraction was the dominant constituent of the settling particulate matter. At the channel site, the lithogenic percentage increased with depth (Fig. 3d and Table 1A). The lithogenic percentage was higher during the autumn–winter period than during the spring–summer period at the three studied depths of this site. This decrease between the two periods was very abrupt at 135 m depth and more gradual at 500 and 692 m depth (Fig. 3d). Maximum lithogenic concentrations occurred in late

December and February. At the open slope site the lithogenic percentage was similar to that from the channel, with maximum values occurring in the same periods (late December and February), and its mean concentration was only slightly higher than that at the channel site (Table 1B). At the canyon site, the lithogenic percentage was higher than that at the channel site (Fig. 3d and Table 1C). In general, the lithogenic percentage in the water column increased with depth, whereas near the bottom it was higher at the canyon and similar at the channel and open slope sites.

#### 4.4. Organic carbon to nitrogen (OC/N)

The OC/N ratio of the collected material is shown in Fig. 5. At the channel site, the mean OC/N ratio during the year increased slightly with depth from 7.7 at 135 m to 8.8 near the bottom. At 135 m depth the

Table 1C

Time-weighted mean fluxes of total mass and major constituents ( $\text{mg m}^{-2} \text{d}^{-1}$ ) and flux-weighted mean concentrations (wt.%) of major constituents of the sinking particles collected in the near-bottom traps installed at the Guadiaro channel and Guadiaro canyon sites between 20 May 1997 and 22 October 1998 (2nd deployment period)

	Channel near-bottom (May 1998–Oct 1998)		Canyon near-bottom (May 1998–Oct 1998)	
	Mean conc.	Mean flux	Mean conc.	Mean flux
TMF	–	795.3	–	6126.6
OC	3	23.9	1.9	114.4
N	0.4	3.2	0.1	8.1
CaCO <sub>3</sub>	11.5	91.8	12.8	786.7
Opal	8.3	66.3	5.5	335.4
Lithogenics	74.1	628.1	77.9	4775.7
<sup>210</sup> Pb*	732.0	0.6	400.0	2.4

\*<sup>210</sup>Pb mean concentration is in  $\text{Bq kg}^{-1}$  and <sup>210</sup>Pb mean fluxes in  $\text{Bq m}^{-2} \text{d}^{-1}$ .



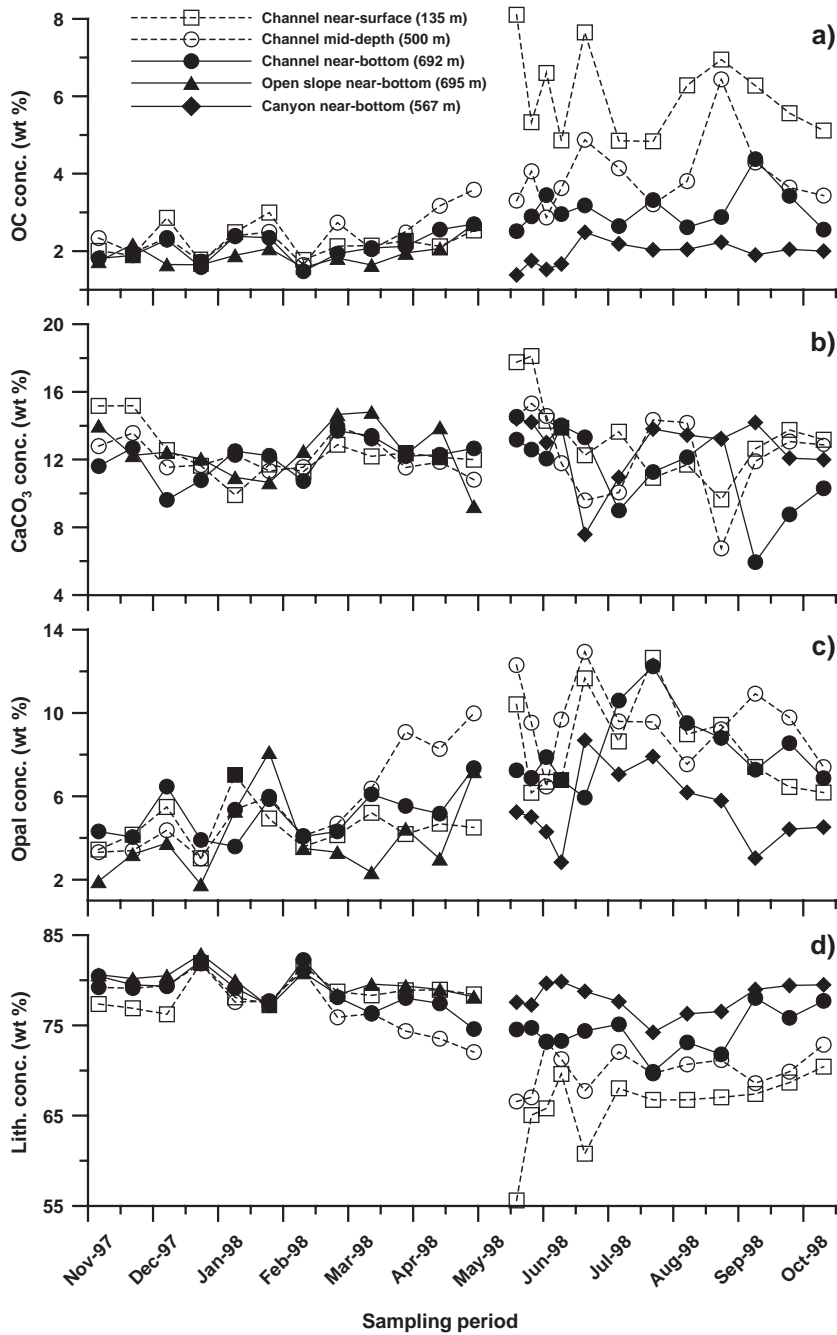


Fig. 3. Time series of major constituent fluxes (a: organic carbon, b: calcium carbonate, c: opal, d: lithogenics) at the three study sites during the deployment period. Near-bottom fluxes are represented by solid lines and mid-depth and near surface fluxes by dashed lines. OC: organic carbon. Lith: lithogenics.

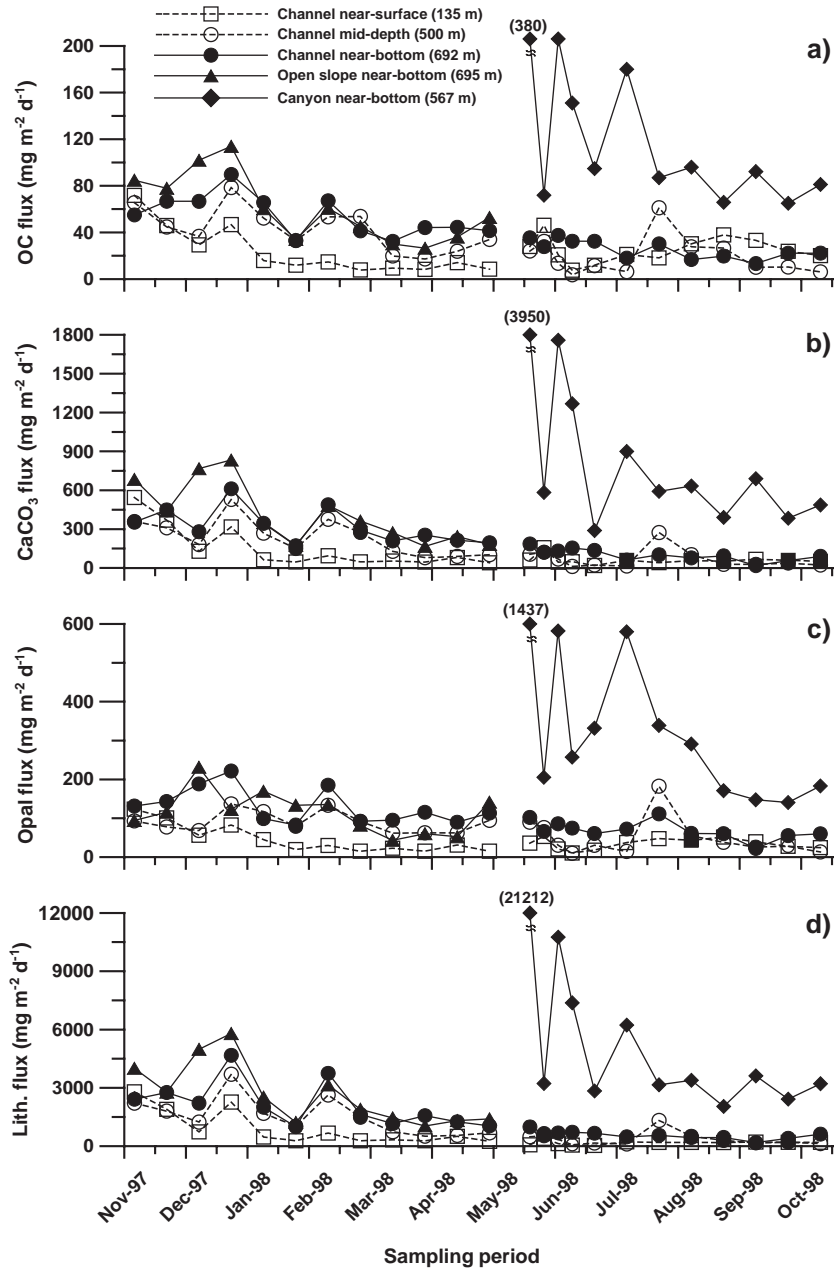


Fig. 4. Time series of major constituents concentrations (a: organic carbon, b: calcium carbonate, c: opal, d: lithogenics) at the three study sites during the deployment period. Near-bottom fluxes are represented by solid lines and mid-depth and near surface fluxes by dashed lines. OC: organic carbon. Lith: lithogenics.

OC/N ratio was more constant in autumn–winter (7.3–8.9) than in summer (5–8.4). The mean OC/N ratios at 500 m depth and near the bottom were similar and although the variability of this ratio at the two

depths was similar, their trends were different. At the open slope site the mean near-bottom OC/N ratio (9.2) was similar to that at the channel site (8.9) and this ratio showed similar variability (7.5–11.2),

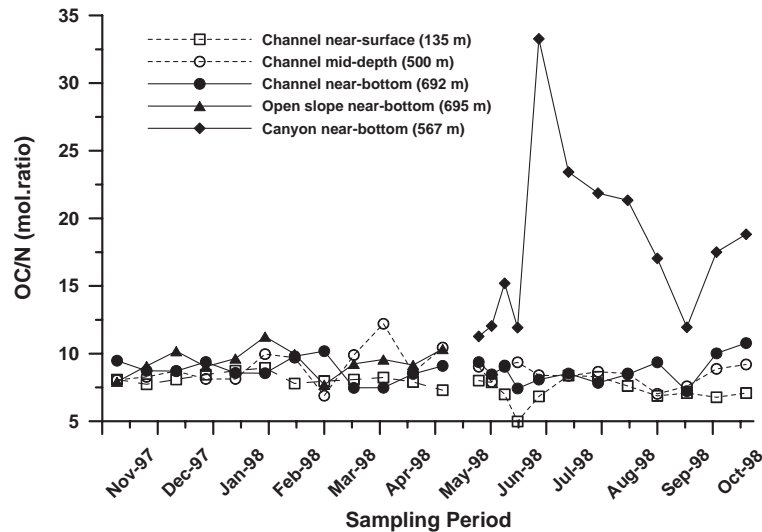


Fig. 5. Time series of OC/N (mol ratio) of the particulate matter collected at the three study sites during the deployment period. Near-bottom fluxes are represented by solid lines and mid-depth and near surface fluxes by dashed lines.

although it followed different trends at these sites. Inside the canyon, the OC/N ratio was much higher than at the other sites (mean ratio 16.54) and it showed a higher variability (11–33) (Fig. 5).

#### 4.5. Lead-210

The  $^{210}\text{Pb}$  concentration in all traps ranged from 291 to 846 Bq kg $^{-1}$ . At the channel site, flux-weighted mean  $^{210}\text{Pb}$  concentration increased slightly with depth (Table 1A) due to scavenging of  $^{210}\text{Pb}$  with settling particles. The  $^{210}\text{Pb}$  concentrations followed a similar trend at all the depths during the year, being lower in winter and increasing during spring and summer (Fig. 6a). Minimum values occurred in February and were similar at the three depths (385–410 Bq kg $^{-1}$ ). Near the bottom there was also a significant decrease in late December. Maximums were also similar at the three depths and occurred at the end of summer. At the open slope site the mean near-bottom  $^{210}\text{Pb}$  concentration was similar to that at the channel site (Table 1B) and the minimum  $^{210}\text{Pb}$  concentration occurred in late December, although in February there was also a significant decrease (Fig. 6a). At the canyon site, the near-bottom  $^{210}\text{Pb}$  concentration was only about half that at the channel site and the minimum values were in late May and mid-June (Fig. 6a; Table 1C).

In general,  $^{210}\text{Pb}$  concentrations showed a more similar variability among traps in winter than in summer and were relatively similar at the channel and open slope sites, but not at the canyon site, where they were significantly lower.  $^{210}\text{Pb}$  fluxes (Fig. 6b) followed the same pattern as the TMF (Fig. 2).

## 5. Discussion

### 5.1. General trends of the downward particles fluxes

In the depositional system of the Guadiaro submarine canyon, near-bottom TMF at the channel and open slope sites was relatively similar whereas it decreased between the canyon and the channel sites. TMF in the water column showed an increasing trend with depth, as has been observed in other submarine canyon studies (Monaco et al., 1990, 1999; Heussner et al., 1999). The temporal evolution of TMF indicates a clear seasonal variation with maximum values in autumn and winter and minimum values in spring and summer (Fig. 2). The fluxes collected at different depths of the channel site show that this trend is more accentuated near the bottom, where the mean TMF of the autumn–winter period is more than 3 times higher than that of the spring–summer period (Tables 1B and C).

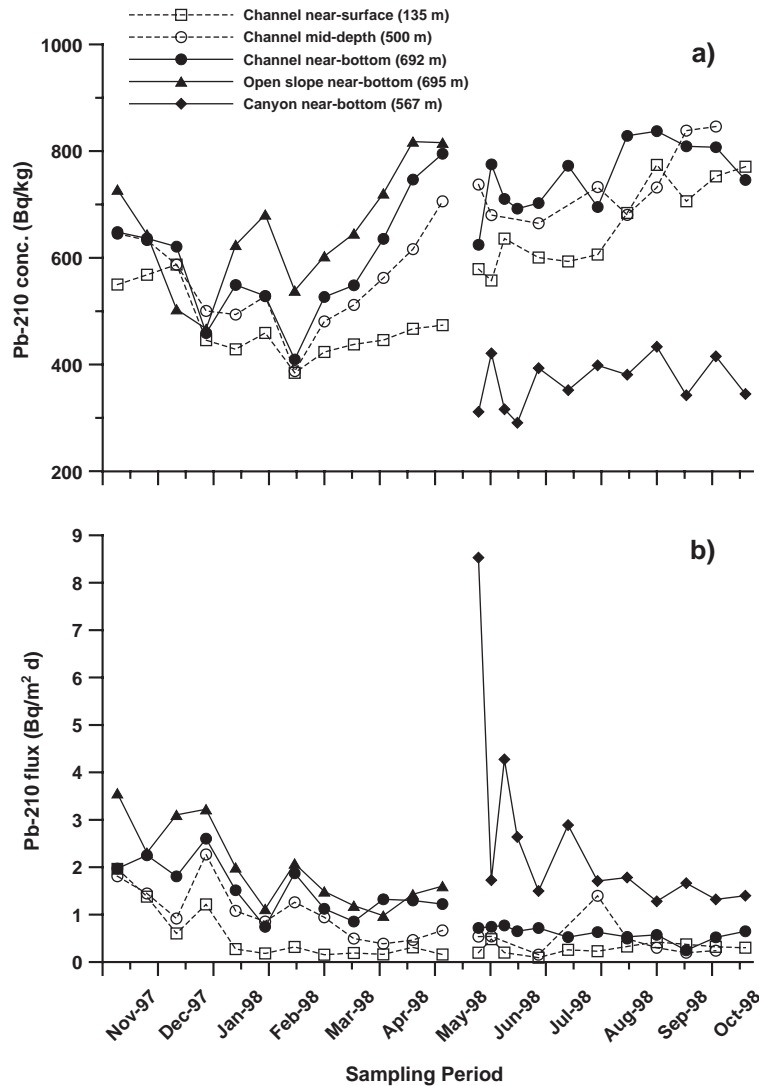


Fig. 6. Time series of  $^{210}\text{Pb}$  concentrations (a) and fluxes (b) of particulate matter collected at the three study sites during the deployment period. Near-bottom fluxes are represented by solid lines and mid-depth and near surface fluxes by dashed lines.

The temporal evolution of major constituents and  $^{210}\text{Pb}$  contents at the channel site also indicates a clear seasonal variation showing higher lithogenic percentages and lower  $^{210}\text{Pb}$  and biogenic constituent concentrations during the autumn–winter period (Figs. 3 and 6). This is consistent with a higher river lithogenic sediment discharge during winter and a faster offshore transfer of resuspended and/or new discharged particles that would lead either to a  $^{210}\text{Pb}$  content dilution or to a lower  $^{210}\text{Pb}$  scavenging during the flood season. In addition, the more similar lithogenics and  $^{210}\text{Pb}$  con-

centrations and trends in winter are coherent with a transfer of more similar particulate matter to near-bottom, mid-depth and near surface waters and probably indicates more active particle matter detachments and lateral transport in the water column during this season.

In spring and summer, the increase in biogenic constituent and  $^{210}\text{Pb}$  concentrations and the decrease in TMF and lithogenics content at the channel site traps (Figs. 3 and 6) suggest a higher influence of primary produced particles with a higher residence time together with a lower lithogenic sediment discharge.

Actually, Moran and Estrada (2001) detected a phytoplankton bloom about 40 miles eastward from the study area with primary production values of about  $1 \text{ g C m}^{-2} \text{ d}^{-1}$  from 1 to 16 May 1998 and Fabres et al., 2002 detected opal and organic matter increases in the sediment trap samples collected nearby in mid-May 1998. Thus, the OC and opal peak observed in May seems to be associated with a biological bloom that could have affected the entire NW Alboran region. Other OC and/or opal peaks that occurred in June, August and September could be associated with other blooms events. The decrease in the OC percentage with depth and the increase in the OC/N ratio with depth in the spring–summer period are due to recycling and remineralisation of organic matter in the water column and to a higher dilution with lithogenic inputs near the bottom. The similar opal concentrations at different depths indicate preservation of biogenic silica during settling in the water column.

Comparison between downward particle fluxes in the Guadiaro depositional system and other studied systems is difficult because of the small size of the Guadiaro submarine canyon, the relatively shallow and proximal area where the canyon ends, and the fact that in the other submarine canyons studied no fluxes were recorded in the channel environment beyond the canyon mouth. However, in general it is possible to say that TMF at the end of the Guadiaro canyon are similar to those measured at the canyon heads (500 m depth) of northwestern Mediterranean canyons (Heussner et al., 1996; Puig and Palanques, 1998), which indicates that TMF in this canyon are relatively important in spite of its small size. TMF at the Guadiaro channel and open slope sites are higher than those on the open slope adjacent to these Mediterranean canyons. This could be due to the narrow shelf of this margin and the proximity of the Guadiaro River mouth to the mooring sites, and also to the lower canyon incision (lower canyon walls) and/or the effect of sediment resuspension by internal waves on the NW Alboran margin (Puig et al., 2004).

### 5.2. The role of river floods and storms in the study area

In the study area, significant river discharge increases took place mainly in winter and the major river floods took place in December and February. On

the other hand, high wave energy events did not occur during the study period. The strongest storm ( $H_s$  of about 3 m) was recorded in February and some small storms ( $H_s$  of about 2 m) occurred in January, May and September (Fig. 7).

The TMF trend is correlated with the Guadiaro river water discharge, showing large increases in winter that coincide with river flood events. In November, relatively high TMF were associated with small increases in the river discharge after the dry season, probably caused by the erosion of the first rain events in the dry watershed of the rivers discharging in the study area (Fig. 7). Afterwards, the stronger TMF peaks during the deployment period were clearly related to the two major river floods that occurred in December and February (Fig. 7a). These flood events produced TMF and lithogenics percentage increases and opal, OC and  $^{210}\text{Pb}$  concentration decreases in all the traps maintaining similar variability in all of them (Figs. 3 and 6). This indicates the influence of simultaneous lateral transport of flood-discharged terrigenous material in most of the water column and not only through the submarine canyon. TMF increases reached higher values near the bottom and, in general, TMF of the sampling periods corresponding to river flood events increased by a factor of 2 with respect to the previous and next sampling periods at the channel and open slope sites. The  $^{210}\text{Pb}$  decrease during the flood periods at all the studied depths is coherent with a more rapid shelf-slope sediment transfer during these events which caused a lower  $^{210}\text{Pb}$  scavenging in the transferred particulate matter.

The most important TMF increases in the study area occurred during the December flood, when the river discharge reached maximum values. The peak of this flood began on December 17th and a high river discharge ( $> 100 \text{ m}^3 \text{ s}^{-1}$ ) lasted until December 24th. At the open slope site, the TMF increase and  $^{210}\text{Pb}$  concentration decrease associated with this flood event affected the third and fourth cups (the change between them was on December 19th), indicating that the flood-induced sediment transfer at this site, began within a time interval of less than 2 days, between December 17th and 19th. However, at the channel site, located 11 miles from the river mouth, the TMF increase and  $^{210}\text{Pb}$  concentration decrease affected only the fourth cup, indicating that the flood-induced sediment transfer reached this site

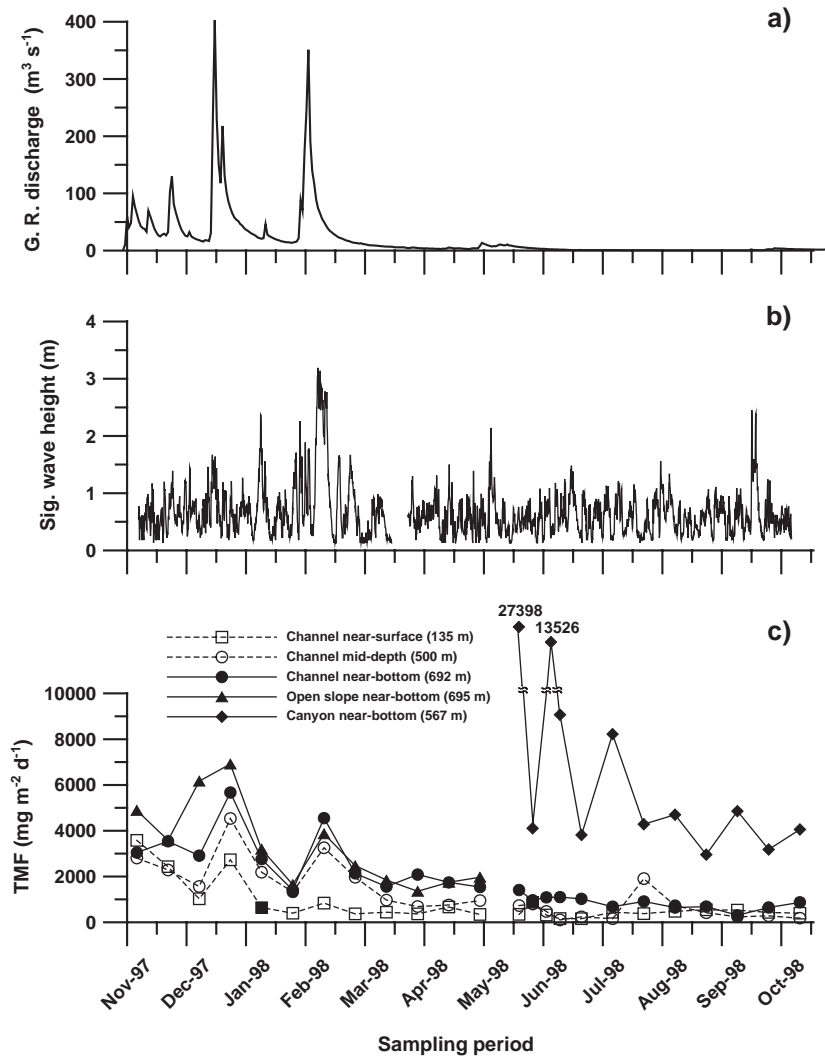


Fig. 7. Temporal variability of the Guadiaro river discharge (a), significant wave height (b) and downward particulate fluxes collected at the three study sites during the deployment period of this study (c). Near-bottom fluxes are represented by solid lines and mid-depth and near surface fluxes by dashed lines.

later, at least two days after the beginning of the flood. In addition, the TMF during the fourth sampling period at the open slope site reached a higher value than that at the channel site (Fig. 7) and, indeed, if the flood-discharged particles had been collected in a single cup, the difference between the two sites would have been much greater. This indicates a more direct transfer of the flood sediment discharge towards the western slope of the Guadiaro Canyon and La Linea Canyon during this event. Thus, the shelf circulation, predominantly directed towards the

Strait of Gibraltar (García Lafuente and Cano Lucaya, 1994), could have generated the higher TMF and lithogenic content and the faster sediment transfer at this site during the flood period.

The second flood began on February 2nd and the river discharge increase lasted until February 8th. In this event, the traps of the channel and the open slope site recorded the TMF increase in the seventh cup, which was open from February 5th to 20th. This means that the particulate matter discharged during this flood reached both study sites at least 3 days after

the beginning of the flood, a little later than during the first flood. During the February flood, the higher near-bottom TMF and the lower  $^{210}\text{Pb}$  concentration at the channel site in comparison with the open slope site suggests a lower direct particle transfer towards the western slope than during the first flood. In addition, the much lower TMF in the 135 m trap of the channel site indicates a more dominant near-bottom particle transfer during the February event. The absence of storms during the December flood could have favoured the advective along-margin transfer towards the Strait of Gibraltar, whereas the storm during the February flood (Fig. 7b) could have induced a more relevant near-bottom cross-margin transport.

In the central part of the western Alboran basin (WAB), 40 miles south-eastward and offshore from the study area, TMF recorded by Fabres et al. (2002) during the first deployment period showed increases related to the same flood events, although they were about three times lower than the peaks recorded in this study and had a delay of 10–20 days in intermediate waters and 20–30 days in near-bottom waters. Furthermore, these authors did not record any TMF increases associated with these floods on the open slope off Malaga, 30 miles eastward from the study area and not incised by submarine canyons. All this indicates that river-flood particle inputs were transferred to the slope of the study area in very few days and towards the centre of the WAB some weeks later.

TMF increases during the February flood were lower than during the December flood, particularly near the surface. The February flood could have discharged less sediment due to lower particle availability on the watershed after the December flood. The storm during the February event could also have caused a greater dispersion of the discharged sediment. In any case, the storm during the second flood did not increase TMF in relation to the first flood, and the other smaller storms did not produce any significant TMF increase during the deployment period either. This suggests that river floods by themselves can play a relevant role in the shelf-slope sediment transfer in this area, where rivers have a very irregular water discharge, the shelf is narrow and the wave regime is not very energetic:  $H_s > 3$  m occurs during less than 0.5% of the time (from the “Puertos del Estado” hydrographic buoys website). The dominant controlling role of river floods on the TMF of the

study area differs from what has been observed in other submarine canyons in which particle flux peaks were mainly controlled by storm events occurring with or without associated river floods (Monaco et al., 1990; Puig et al., 2003; Palanques et al., 2005).

### 5.3. Fluxes inside the canyon. The role of trawling activities and internal waves

At the canyon site, the very strong TMF peaks ( $> 10,000 \text{ mg m}^{-2} \text{ d}^{-1}$ ) coinciding with the lowest  $^{210}\text{Pb}$  concentrations ( $< 350 \text{ Bq kg}^{-1}$ ) and highest OC/N ratios (Figs. 2, 5 and 6) in May and June, in absence of river floods or significant storm events, indicate a strong local resuspension nearby. These sudden and sporadic increases were not observed at the channel site and cannot be explained by natural processes. The fact that the mooring at the canyon site was caught by a fishing boat during the first deployment suggests that trawling activities could have generated these strong TMF peaks. Similar peaks interpreted as caused by trawling have been observed in other submarine canyons (Puig and Palanques, 1998; Palanques et al., 2005).

Independently of these peaks, near-bottom TMF at the Guadiaro canyon site maintained values 5 to 10 times higher than those at the channel site during the whole spring–summer period, indicating the presence of a continuous mechanism enhancing TMF inside the canyon. In addition, the constant higher OC/N ratio (1.5 to 5 times that of the channel), higher lithogenics content, lower  $^{210}\text{Pb}$  concentration (half that of the channel), and lower OC and opal concentrations at the canyon site, without the occurrence of any flood or storm event, suggest that a large part of the particulate matter may come from sediment resuspended by a continuously active process such as internal waves focused along the canyon axis. This process was identified by the study of the nepheloid structure and the currents and turbidity temporal series in this canyon (Puig et al., 2004). This study revealed the development of a thick near-bottom nepheloid layer (170 m thick near the canyon mooring site) that extended up to 600 m depth and was generated by internal wave resuspension. These authors also determined that the net transport of near-bottom currents at the canyon site was almost null which favoured the settling of particles resuspended along the canyon

axis. These observations and the recorded TMF suggest that this submarine canyon works as a natural sediment trap and this behaviour explains the strong TMF differences recorded between the canyon and the channel sites.

This near-bottom nepheloid layer that developed along the canyon did not reach the channel and the open slope sites but internal wave activity also created detachments of intermediate nepheloid layers at about 300 m depth that could extend more seaward than the near-bottom nepheloid layer (Puig et al., 2004). The isolated peak in the 500 m depth trap of the channel site in August indicates that intermediate nepheloid layers can reach this site sporadically. Sediment resuspension by internal waves in submarine canyons has also been suggested to occur in other submarine canyons that showed a similar suspended matter distribution and downward particle flux pattern (e.g., Gardner, 1989).

The channel and open slope sites received similar particle inputs, both in composition and amount, and in fact the open slope site received slightly higher particles inputs than the channel because it can also receive inputs from the western slope and La Linea submarine Canyon. This suggests that the channel receives only unconfined sediment like the open slope region and that the retention of resuspended material inside the canyon contributes to it. Both sites receive only the particles that manage to overflow the canyon walls, that are detached from the canyon axis or that are transferred directly through the open slope waters.

## 6. Conclusions

The Guadiaro canyon works as a natural trap retaining high TMF that include sediment periodically resuspended by internal waves and sediment resuspended occasionally by trawling. The Guadiaro channel did not work as a preferential conduit of sediment during the deployment period and received considerably lower TMF than those of the canyon and similar unconfined particle fluxes to those of the open slope site. In the water column of the channel site TMF increased with depth and had a seasonal variation showing maximum values in autumn and winter and minimum values in spring and summer.

River flood events controlled the high winter TMF in the study area. These events generated a rapid

lateral sediment transport in the entire slope water column producing TMF and lithogenics percentage increases and Opal, OC and  $^{210}\text{Pb}$  concentration decreases in all the traps. The flood-sediment inputs reached the open slope and channel sites at least between 1 and 3 days after the beginning of the floods and the central part of the WAB between 10 and 20 days later. In the study area, usual storm events are not strong enough to generate major shelf-slope transport events, and river floods by themselves play a very relevant role in the shelf-slope sediment transfer.

## Acknowledgements

This study was supported by the “FLUXALB” project funded by the “Comisión Interministerial de Ciencia y Tecnología”, ref. MAR96-1781-CO2-01 and by the “CANYON” project funded by the “Dirección General de Enseñanza Superior e Investigación Científica”, ref. MAR99-1060-CO3-01. We thank the officers and crew of the R/V “García del Cid” for their help and dedication during the three FLUXALB cruises. We also thank the “Confederación Hidrográfica del Sur” for providing the Guadiaro River discharge data and “Puertos del Estado” for kindly providing the current meter and hydrographic buoy data. We would like to thank Neus Maestro and Benedicta Paracuellos for their help during trap sample preparation and analysis. IAEA-MEL operates under a bilateral agreement between the IAEA and the Government of the Principality of Monaco.

## References

- Alonso, B., Ercilla, G., 2003. Small turbidite systems in a complex tectonic setting (SW Mediterranean Sea): morphology and growth patterns. *Mar. Pet. Geol.* 19, 1225–1240.
- Baldacci, A., Corsini, G., Grasso, R., Manzella, G., Allen, J.T., Cipollini, P., Guymer, T.H., Snaith, H.M., 2001. A study of the Alboran Sea mesoscale system by means of empirical orthogonal functions decomposition of satellite data. *J. Mar. Syst.* 29, 293–311.
- Biscaye, P.E., Anderson, R.F., 1994. Fluxes of particulate matter on the slope of the southern Middle Atlantic Bight: SEEP-II. *Deep-Sea Res.* 41, 459–509.
- Biscaye, P.E., Anderson, R.F., Deck, B.L., 1988. Fluxes of particles and constituents to the eastern United State continental slope and rise: SEEP-I. *Cont. Shelf Res.* 8, 855–904.



- Copin-Montegut, G., Avril, B., 1993. Vertical distribution and temporal variation of dissolved organic carbon in the North-Western Mediterranean Sea. *Deep-Sea Res.* 40, 1963–1972.
- Dachs, J., Bayona, J.M., Fowler, S.W., Miquel, J.C., Albaiges, J., 1996. Vertical fluxes of polycyclic aromatic hydrocarbons and organochlorine compound in the western Alboran Sea (Southern Mediterranean). *Mar. Chem.* 52, 75–86.
- Dachs, J., Bayona, J.M., Fowler, S.W., Miquel, J.C., Albaiges, J., 1998. Evidence for cyanobacterial inputs and heterotrophic alteration of lipids in sinking particles in the Alboran Sea (SW Mediterranean). *Mar. Chem.* 60, 189–201.
- Dafner, E.V., Sempéré, R., Bryden, H.L., 2001. Total organic carbon distribution and budget through the Strait of Gibraltar in April 1998. *Mar. Chem.* 73, 233–252.
- De Lazzari, A., Boldrin, A., Rabitti, S., Turchetto, M.M., 1999. Variability and downward fluxes of particulate matter in the Otranto Strait area. *J. Mar. Syst.* 20, 399–413.
- Deuser, W.G., 1986. Seasonal and interannual variations in deep-water particle fluxes in the Sargasso Sea and their relation to surface hydrography. *Deep-Sea Res.* 33, 225–246.
- Ercilla, G., Alonso, B., Baraza, J., 1992. Quaternary Sedimentary evolution of the northwestern Alboran Sea. *Geo Mar. Lett.* 12, 144–149.
- Fabres, J., Calafat, A., Sanchez-Vidal, A., Canals, M., Heussner, S., 2002. Composition and spatio-temporal variability of particle fluxes in the Western Alboran Gyre, Mediterranean Sea. *J. Mar. Syst.* 33–34, 197–214.
- García-Gorrioz, E., Carr, M.E., 1999. The climatological annual cycle of satellite-derived phytoplankton pigments in the Alboran Sea. *Geophys. Res. Lett.* 19, 2985–2988.
- García Lafuente, Cano Lucaya, N., 1994. Tidal dynamics and associated features of the northwestern shelf of the Alboran Sea. *Cont. Shelf Res.* 14, 1–21.
- Gardner, W.D., 1989. Baltimore canyon as a modern conduit of sediment to the deep sea. *Deep-Sea Res.* 36, 323–358.
- Gardner, W.D., Biscaye, P.E., Richardson, M.J., 1997. A sediment trap experiment in the Vema Channel to evaluate the effect of horizontal particle fluxes on measured vertical fluxes. *J. Mar. Res.* 55, 995–1028.
- Gil, J., Gomiz, D., 1994. Circulación geostrofica, dinámica de mesoescala y fertilización de aguas someras en el sector norte del Mar de Alborán. *Bol. Inst. Esp. Oceanogr.* 95, 95–117.
- Heburn, G.W., La Violette, P.E., 1990. Variations in the structure of the anticyclonic gyres found in the Alboran Sea. *J. Geophys. Res.* 95, 1599–1613.
- Heussner, S., Carbonne, J., Ratti, C., 1990. The time-series sediment trap and the trap processing techniques used during the ECOMARGE experiment. *Cont. Shelf Res.* 9–11, 943–958.
- Heussner, S., Calafat, A., Palanques, A., 1996. Quantitative and qualitative features of particle fluxes in the North-Balearic Basin. In: Canals, M., Casamor, J.L., Cacho, I., Calafat, A., Monaco, A. (Eds.), *EUROMARGE-NB Final Report. MAST II Programme, EU*, pp. 41–66.
- Heussner, S., Durrieu de Madron, X., Radakovitch, O., Beaufort, L., Biscaye, P.E., Carbonne, J., Delsaut, N., Etcheber, H., Monaco, A., 1999. Spatial and temporal patterns of downward particle fluxes on the continental slope of the Bay of Biscay (north-eastern Atlantic). *Deep-Sea Res.* 46, 2101–2146.
- Masqué, P., Fabres, J., Canals, M., Sánchez-Cabeza, J.A., Sánchez-Vidal, A., Cacho, I., Calafat, A.M., Bruach, J.M., 2003. Accumulation rates of major constituents of hemipelagic sediments in deep Alborán Sea: a centennial perspective of sediment dynamics. *Mar. Geol.* 193, 207–233.
- Millot, C., 1999. Circulation in the western Mediterranean Sea. *J. Mar. Syst.* 20, 423–442.
- Monaco, A., Courp, T., Heussner, S., Carbonne, J., Fowler, S.W., Deniaux, B., 1990. Seasonality and composition of particulate fluxes during ECOMARGE-I western Gulf of Lions. *Cont. Shelf Res.* 9–11, 959–987.
- Monaco, A., Durrieu de Madron, X., Radakovitch, O., Heussner, S., Carbonne, J., 1999. Origin and variability of downward biogeochemical fluxes on the Rhone continental margin (NW Mediterranean). *Deep-Sea Res.* 46, 1483–1511.
- Moran, X.A.G., Estrada, M., 2001. Short-term variability of photosynthetic parameters and particulate and dissolved primary production in the Alborán Sea (SW Mediterranean). *Mar. Ecol., Progr. Ser.* 212, 53–67.
- Mortlock, R.A., Froelich, P.N., 1989. A simple method for the rapid determination of biogenic opal in pelagic sediments. *Deep-Sea Res.* 36, 1415–1426.
- Packard, T.T., Minas, H.J., Coste, B., Martinez, R., Bonn, M.C., Gostan, J., Garfield, P., Christensen, J., Dortch, Q., Minas, M., Copping-Montegut, G., Copping-Montegut, C., 1988. Formation of the Alboran minimum zone. *Deep-Sea Res.* 35, 1111–1118.
- Palanques, A., Isla, E., Puig, P., Sanchez-Cabeza, J.A., Masqué, P., 2002. Annual evolution of downward particle fluxes in the western Bransfield Strait (Antarctica) during the FRUELA experiment. *Deep-Sea Res.* 49, 903–920.
- Palanques, A., García-Ladona, E., Gomis, D., Martín, J., Marcos, M., Pascual, A., Puig, P., Emelianov, M., Guillén, J., Gili, J.M., Tintoré, J., Jordi, A., Basterretxeab, G., Font, J., Segura, M., Blasco, D., Monserrat, S., Ruiz, S., Pagés, F., 2005. General patterns of circulation, sediment fluxes and ecology of the Palamós (La Fonera) submarine canyon, north-western Mediterranean. *Prog. Oceanogr.* 66 (2–4), 89–119.
- Peinert, R., Miquel, J.C., 1994. The significance of frontal processes for vertical particle fluxes: a case study in the Alboran Sea (SW Mediterranean Sea). *J. Mar. Syst.* 5, 377–389.
- Puig, P., Palanques, A., 1998. Temporal variability and composition of settling particle fluxes on the Barcelona continental margin. *J. Mar. Res.* 56, 639–654.
- Puig, P., Ogston, A.S., Mullenbach, B.L., Nittrouer, C.A., Sternberg, R.W., 2003. Shelf-to-canyon sediment-transport processes on the Eel continental margin (northern California). *Mar. Geol.* 193, 129–149.
- Puig, P., Palanques, A., Guillén, J., El Khatib, M., 2004. The role of internal waves in the generation of nepheloid layers in the northwestern Alboran slope: implications for continental margin shaping. *J. Geophys. Res.* 109 (C09011-11 pp)
- Rodríguez, V., Echevarría, F., Rodríguez, J., Jiménez-Gómez, F., Bautista, B., 1994. Nutrientes, fitoplancton, bacterias y material particulado del mar de Alborán, en Julio de 1992. Informe Técnico. Instituto Español de Oceanografía 146 (4), 53–79.

- Rodríguez, J., Blanco, J.M., Jiménez-Gómez, F., Echavarría, F., Gil, J., Rodríguez, V., Ruiz, J., Bautista, B., Guerrero, F., 1998. Patterns in the size structure of the phytoplankton community in the deep fluorescence maximum of the Alboran Sea (southwestern Mediterranean). *Deep-Sea Res.* 45, 1577–1593.
- Rubin, J.P., Gil, J., Ruiz, J., Cortés, M.D., Jiménez-Gómez, F., Parada, M., Rodríguez, J., 1992. La distribución ictioplanctónica y su relación con parámetros físicos químicos y biológicos en el sector norte del mar de Alborán, en Julio de 1991. (Resultados de la campaña Ictio.Alborán 0791). Informe Técnico. Instituto Español de Oceanografía 139, 1–49.
- Sánchez-Cabeza, J.A., Masqué, P., Ani-Ragolta, I., 1998.  $^{210}\text{Pb}$  and  $^{210}\text{Po}$  analysis in sediments and soils by microwave acid digestion. *J. Radioanal. Nucl. Chem.* 227, 19–22.
- Sarhan, T., Lafuente, J.G., Vargas, M., Vargas, J.M., Plaza, F., 2000. Upwelling mechanisms in the northwestern Alboran Sea. *J. Mar. Syst.* 23, 317–331.
- Thunel, R.C., 1998. Seasonal and annual variability in particle fluxes in the Gulf of California: a response to climate forcing. *Deep-Sea Res.* 45, 2059–2083.
- Tintoré, J., Gomis, D., Alonso, S., Parilla, G., 1991. Mesoscale dynamics and vertical motion in the Alboran Sea. *J. Phys. Oceanogr.* 18, 643–656.
- Viúdez, A., Tintoré, J., Haney, R., 1996. Circulation in the Alborán Sea as determined by quasi-synoptic hydrographic observations: Part I. Three-dimensional structure of the two anticyclonic gyres. *J. Phys. Oceanogr.* 26, 684–705.
- Walsh, J.J., 1991. Importance of continental margins in the marine biogeochemical cycling of carbon and nitrogen. *Nature* 350, 5–53.
- Walsh, J.J., Biscaye, P.E., Csanady, G.T., 1988. The 1983–1984 Shelf Edge Exchange Processes (SEEP)-I experiment: hypotheses and highlights. *Cont. Shelf Res.* 8, 435–456.
- Walsh, J.P., Nittrouer, C.A., 1999. Observations of sediment flux to the Eel continental slope, northern California. *Mar. Geol.* 154, 55–68.